Inorganic Chemistry
Article

Inorg. Chem. **2010**, *49*, 9649–9654 **9649**
DOI: 10.1021/ic101371z

The Topotactic Reduction of $Sr_3Fe_2O_5Cl_2$—Square Planar Fe(II) in an Extended Oxyhalide

Edward Dixon and Michael A. Hayward*

Department of Chemistry, University of Oxford, Inorganic Chemistry Laboratory, South Parks Road, Oxford, OX1 3QR, United Kingdom

Received July 9, 2010

The topotactic reduction of the oxychloride $Sr_3Fe_2O_5Cl_2$ with LiH results in the formation of $Sr_3Fe_2O_4Cl_2$. Neutron powder diffraction data show that $Sr_3Fe_2O_4Cl_2$ adopts a body-centered tetragonal crystal structure (*I*4/*mmm*, *a* = 4.008(1) Å, *c* = 22.653(1) Å at 388 K) with anion vacancies located within the SrO layer of the phase. This leads to a structure consisting of infinite sheets of corner-sharing $Fe(II)O_4$ square planes. Variable-temperature neutron diffraction data show that $Sr_3Fe_2O_4Cl_2$ adopts G-type antiferromagnetic order below $T_N \sim 378(10)$ K with an ordered moment of 2.81(9) μ_B per iron center at 5 K consistent with the presence of high-spin Fe(II). The observed structural and chemical selectivity of the reduction reaction is discussed. The contrast between the structure of $Sr_3Fe_2O_4Cl_2$ and the isoelectronic all-oxide analogue ($Sr_3Fe_2O_5$) suggests that by careful selection of substrate phases, the topotactic reduction of complex transition metal oxychlorides can lead to the preparation of novel anion-deficient phases with unique transition metal−oxygen sublattices which cannot be prepared via the reduction of all-oxide substrates.

Introduction

Complex transition metal oxides and related mixed anion phases are of great importance from an academic and technological perspective due to the diverse array of physical properties they exhibit. These properties typically arise from the cooperative behavior of electrons located in partially filled d states. By modifying the valence electron count (metal oxidation state), local metal coordination (crystal field effects), and long-range cation−anion−cation connectivity (exchange pathways), chemists can tune and manipulate the behavior of these electrons and thus the physical behavior of these materials. Conventionally, such physical property tuning has been achieved via selective cation substitutions, which readily modify transition metal oxidation states and valence electron counts. However there is growing interest in tuning the physical behavior of solids containing transition metals by manipulating their anion lattices because this not only changes the electron count (through reduction or oxidation) but can also modify the local transition metal coordination sphere and the long-range cation−anion−cation connectivity, potentially leading to more dramatic changes in physical behavior.

Recently, we have demonstrated that binary metal hydrides can be used as powerful solid state reducing agents for the low-temperature deintercalation of oxide ions (topotactic reduction) from complex transition metal oxides to yield new phases with novel transition metal oxidation states and unusual local coordinations.[1−3] In order to reap the full benefit of this synthetic approach and achieve a situation where the directed synthesis of target phases is possible, it is necessary to control which of the various anions in a substrate phase are removed and how the resulting anion vacancies order.

One strategy to exert such control over topotactic reduction reactions utilizes the strong interaction between the anion and cation lattices in complex oxides to direct the progress and products of anion deintercalation reactions. For example, the reduction of the isostructural and isoelectronic A-cation ordered phases $YBaCo_2O_5$ and $LaBaCo_2O_5$ with NaH yields $YBaCo_2O_{4.5}$ and $LaBaCo_2O_{4.25}$, respectively.[4] These two reduced phases have different anion contents and anion vacancy ordering patterns, despite starting from isostructural substrate phases, demonstrating the directing influence of the A cations in this case. Building on this observation, we have sought to investigate the directing influences of heteroanions on the progress of topotactic reductions in mixed anion solids. Here, we describe the first topotactic reduction of a complex oxyhalide, $Sr_3Fe_2O_5Cl_2$, an $n = 2$ Ruddlesden−Popper phase with a structure analogous to $Sr_3Fe_2O_7$ (Figure 1). Reaction of $Sr_3Fe_2O_5Cl_2$ with LiH yields $Sr_3Fe_2O_4Cl_2$, a phase which contains sheets of

*To whom correspondence should be addressed. Tel.: +44 1865 272623. Fax: +44 1865 272690. E-mail: michael.hayward@chem.ox.ac.uk.

(1) Hayward, M. A.; Green, M. A.; Rosseinsky, M. J.; Sloan, J. *J. Am. Chem. Soc.* **1999**, *121*, 8843–8854.
(2) Adkin, J. J.; Hayward, M. A. *J. Solid State Chem.* **2006**, *179*, 70–76.
(3) Hayward, M. A. *Chem. Mater.* **2005**, *17*, 670–675.
(4) Seddon, J.; Suard, E.; Hayward, M. A. *J. Am. Chem. Soc.* **2010**, *132*, 2802–2810.

Published on Web 09/14/2010

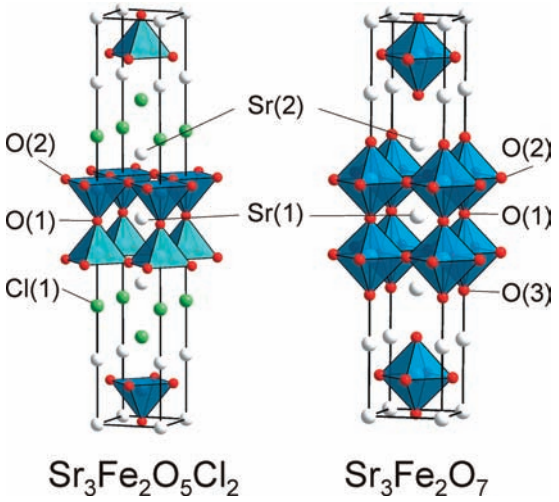

Figure 1. The crystal structures of the $n=2$ Ruddlesden−Popper phases $Sr_3Fe_2O_5Cl_2$ and $Sr_3Fe_2O_7$.

square-planar Fe(II) centers, providing a structural contrast to the recently reported phases $SrFeO_2$ and $Sr_3Fe_2O_5$, which contain similar iron coordination sites.[5,6]

Experimental Section

Preparation of $Sr_3Fe_2O_5Cl_2$. Samples of $Sr_3Fe_2O_5Cl_2$ were prepared by a direct-combination route that has previously been described by Weller et al.[7] Suitable quantities of SrO (prepared by the decomposition of $SrCO_3$ at 1100 °C under vacuum), $SrCl_2$ (dried at 180 °C under vacuum), and Fe_2O_3 (Alfa Aesar, 99.99%) were thoroughly mixed with an agate pestle and mortar in an argon-filled glovebox (O_2 and H_2O levels < 1 ppm). The mixture was then heated in an evacuated silica ampule at 850 °C for 2 periods of 24 h with one intermediate grinding. X-ray powder diffraction data collected from this material were consistent with a single phase with lattice parameters $a = 3.947(1)$ Å and $c = 23.786(1)$ Å in good agreement with previously reported values ($a = 3.946(1)$ Å, $c = 23.786(1)$ Å).[7]

Reduction of $Sr_3Fe_2O_5Cl_2$. The reduction of $Sr_3Fe_2O_5Cl_2$ was performed using LiH as a solid state reducing agent.[8] Small samples (~300 mg) of $Sr_3Fe_2O_5Cl_2$ were ground together in a 1:4 molar ratio with LiH in an argon-filled glovebox. These mixtures were then sealed under vacuum in Pyrex ampules and heated at temperatures between 210 and 400 °C to monitor the temperature dependence of the reduction reaction. Due to the hazards associated with the production of hydrogen gas when using LiH as a reducing agent,[8] large-scale samples suitable for characterization by neutron powder diffraction were prepared by means of a spring-loaded venting apparatus described previously.[9] Approximately 4 g of $Sr_3Fe_2O_5Cl_2$ was mixed in a 1:4 molar ratio with LiH and heated at 350 °C for 4 periods of 24 h with intermediate grinding. The sample was then heated for a further 48 h in an evacuated Pyrex ampule. After reaction, the sample was washed under nitrogen with 4 × 100 mL of methanol to remove any lithium-containing phases (LiH and Li_2O) before being dried under vacuum.

Characterization. X-ray powder diffraction data were collected using a PANalytical X'Pert diffractometer incorporating an X'celerator position-sensitive detector (monochromatic Cu Kα1 radiation). Data were collected from air-sensitive samples under an inert atmosphere using a homemade gas-tight sample holder. Electron diffraction patterns were collected from samples supported on lacy carbon grids (deposited from suspension in chloroform) using a JEOL 2000FX microscope operating at 200 kV. Neutron powder diffraction data were collected in the temperature range $5 < T/\mathrm{K} < 300$ from samples contained in vanadium cans, sealed under argon with indium washers, at a wavelength of $\lambda = 1.59$ Å using the D2b diffractometer (ILL neutron source, Grenoble, France). Additional data sets were collected in the temperature range $300 < T/\mathrm{K} < 388$ using the POLARIS diffractometer (ISIS neutron source, U.K.) from samples contained in vanadium cans sealed under argon using a copper gasket. Rietveld profile refinement was performed using the GSAS suite of programs.[10] Average iron oxidation states in all phases were determined by iodiometric titration. Approximately 50 mg of material was placed in a three-necked flask under an argon atmosphere. The solid was then dissolved in 1.1 M HCl containing an excess of KI, and the liberated I_2 was titrated with previously standardized $Na_2S_2O_3$ under an argon purge to prevent oxidation by the air. Titrations were repeated three times or until a consistent result was obtained.

Results

Reactivity of $Sr_3Fe_2O_4Cl_2$. X-ray powder diffraction data collected from the products of the reaction between $Sr_3Fe_2O_5Cl_2$ and LiH reveal that at temperatures below 350 °C no reaction occurs. Reactions performed at temperatures above 400 °C result in the decomposition of the ternary oxychloride phase and the formation of Sr_2FeO_3Cl, elemental iron, and $LiFeO_2$. In the temperature range $350 < T/°\mathrm{C} < 400$, reactions resulted in the formation of a body-centered tetragonal phase consistent with the topotactic reduction of $Sr_3Fe_2O_5Cl_2$.

Structural Characterization. X-ray powder diffraction data collected from the washed product of the reaction between $Sr_3Fe_2O_5Cl_2$ and LiH at 350 °C could be readily indexed on the basis of a body-centered tetragonal unit cell ($a = 4.009(1)$ Å, $c = 22.638(1)$ Å) consistent with the topotactic reduction of $Sr_3Fe_2O_5Cl_2$ to a phase of composition $Sr_3Fe_2O_{5-x}Cl_2$. In contrast to the X-ray powder diffraction data, neutron powder diffraction data collected at room temperature from $Sr_3Fe_2O_{5-x}Cl_2$ exhibited a series of large d-spacing diffraction features which are inconsistent with the simple body-centered tetragonal cell described above (Figure 2). These additional diffraction features could be indexed using a unit cell related to the X-ray cell by an $a' = \sqrt{2}a$, $b' = \sqrt{2}b$, $c' = c$ geometric expansion. In order to confirm the size and symmetry of the crystallographic unit cell, electron diffraction data were collected. As can be seen in Figure 3, these data could be readily indexed using the body-centered tetragonal cell determined from the X-ray powder diffraction data, suggesting the additional features observed in the neutron diffraction data are due to magnetic order. This was further confirmed by the observation that the

(5) Tsujimoto, Y.; Tassel, C.; Hayashi, N.; Watanabe, T.; Kageyama, H.; Yoshimura, K.; Takano, M.; Ceretti, M.; Ritter, C.; Paulus, W. *Nature* **2007**, *450*, 1062–1065.
(6) Hiroshi, K.; Takashi, W.; Yoshihiro, T.; Atsushi, K.; Yuji, S.; Kazuyoshi, K.; Kazuyoshi, Y.; Naoaki, H.; Shigetoshi, M.; Mikio, T.; Monica, C.; Werner, P.; Clemens, R.; Gilles, A. *Angew. Chem.* **2008**, *47*, 5740–5745.
(7) Dann, S. E.; Weller, M. T.; Currie, D. B. *J. Solid State Chem.* **1992**, *97*, 179–185.
(8) Adkin, J. J.; Hayward, M. A. *Inorg. Chem.* **2008**, *47*, 10959–10964.
(9) O'Malley, M.; Lockett, M. A.; Hayward, M. A. *J. Solid State Chem.* **2007**, *180*, 2851–2858.
(10) Larson, A. C.; Von Dreele, R. B. *General Structure Analysis System*, Los Alamos National Laboratory Report LAUR 86−748, Los Alamos National Laboratory: Los Alamos, NM, **2000**.

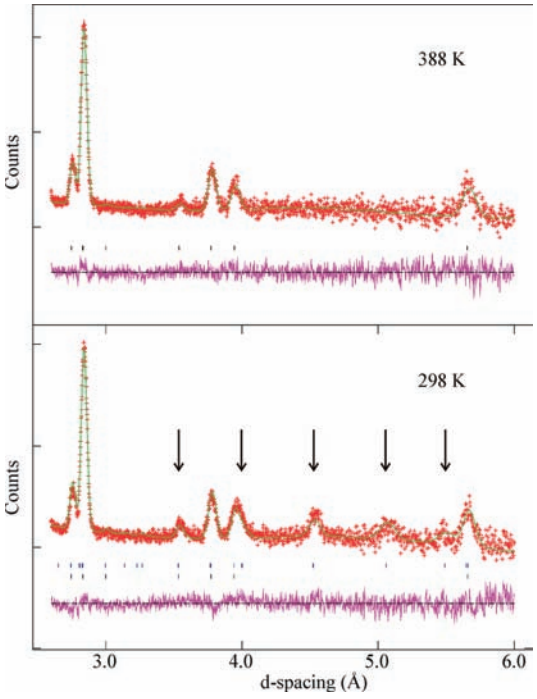

Figure 2. Observed, calculated, and difference plots from the structural refinement of $Sr_3Fe_2O_4Cl_2$ at 388 K (top) and structural and magnetic refinement at 298 K (bottom) against neutron powder diffraction data. The major magnetic reflections are marked with arrows.

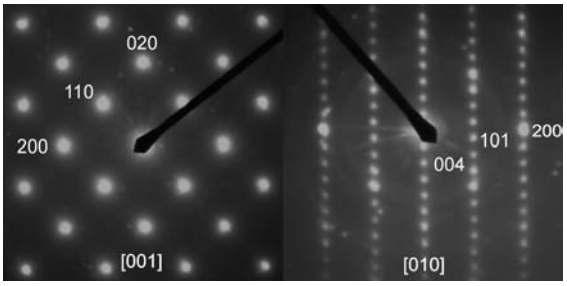

Figure 3. Electron diffraction data collected from the [001] and [010] zone axes of $Sr_3Fe_2O_4Cl_2$ consistent with a tetragonal unit cell: a = 4.008 Å, c = 22.653 Å.

intensities of these additional neutron diffraction features diminish with increasing temperature such that, at 388 K, their intensity was zero (Figure 2), consistent with a loss of magnetic order at this temperature.

To avoid the complications of simultaneous structural and magnetic refinements, the structural refinement of $Sr_3Fe_2O_{5-x}Cl_2$ was performed against neutron powder diffraction data collected at 388 K. A structural model based on that of $Sr_3Fe_2O_5Cl_2$ was refined against this data set. During the refinement, all atomic positional and thermal parameters were allowed to vary, and to account for the nonstoichiometry of the reduced phase, the fractional occupancies of the anion sites were also allowed to vary. The occupancy of the O(1) "bridging axial" anion site (Figure 1) rapidly declined to zero within error with an associated improvement in the fit to the data. In the final stages of the refinement, the fractional occupancies of all of the atomic sites were allowed to vary, but all other atomic positions remained fully occupied within error, indicating a composition of $Sr_3Fe_2O_4Cl_2$. Close

Table 1. Refined Structural Parameters of $Sr_3Fe_2O_4Cl_2$ at 388 K

atom	Wyckoff position	x	y	z	U_{iso} (Å^3)
Sr(1)	2*a*	0	0	0	0.0036(5)
Sr(2)	4*e*	0	0	0.153(1)	0.0038(4)
Fe(1)	4*e*	0	0	0.425(1)	0.0028(2)
O(2)	8*g*	0.5	0	0.078(1)	0.0058(2)
Cl(1)	4*e*	0	0	0.294(1)	0.0087(2)

$Sr_3Fe_2O_4Cl_2$: space group, $I4/mmm$; a = 4.008(1) Å; c = 22.653(1) Å; cell volume = 364.01(1) Å^3; weight fraction = 91.9(1)%
Fe: space group, $Im\bar{3}m$; a = 2.866(1) Å; cell volume = 23.554(3) Å^3; weight fraction = 8.1(1)%
χ^2 = 1.858, wR_p = 2.14%, R_p = 3.77%

Table 2. Selected Bond Lengths and Bond Valence Parameters from the Refined Structure of $Sr_3Fe_2O_4Cl_2$

cation	anion	bond length (Å)	BVS contribution	total BVS
Fe(1)	O(2)	4 × 2.006(1)	4 × 0.479	2.002
	Cl(1)	1 × 2.977(2)	1 × 0.079	
Sr(1)	O(2)	8 × 2.674(1)	8 × 0.223	1.780
Sr(2)	O(2)	4 × 2.632(2)	4 × 0.249	2.031
	Cl(1)	4 × 3.072(1)	4 × 0.219	
		1 × 3.192(2)	1 × 0.158	

inspection of the data revealed a set of weak diffraction reflections consistent with the presence of metallic iron. A structural description of this phase was added to the refinement model, which readily converged to give a good statistical fit to the data (χ^2 = 1.858). Full details of the refined structural parameters are given in Table 1 with selected bond lengths from the refined structure of $Sr_3Fe_2O_4Cl_2$ shown in Table 2. Plots of the observed and calculated data are shown in the Supporting Information. In order to confirm the refined composition, iodiometric titrations were performed, the results of which are consistent with an average iron oxidation state of +2 for the bulk phase. Due to the highly air-sensitive nature of $Sr_3Fe_2O_4Cl_2$, it was not possible to confirm the stoichiometry of the phase using reoxidative thermogravimetric analysis. Indeed, bulk samples of this material are pyrophoric, and extreme care should be taken when handling this material.

Magnetic Characterization. Neutron powder diffraction data collected at 5 K show additional features relative to the 388 K data set which were assigned to magnetic order, as described above. A series of magnetic ordering models consistent with the crystallographic symmetry were compared to the 5 K data, and the best fit was obtained by a simple G-type antiferromagnetic model with moments aligned parallel to the z axis (Figure 4a). The refinement converged readily to yield an ordered moment of 2.81(9) μ_B per iron center at 5 K. Complete details of the magnetic refinement and plots of observed and calculated data are shown in the Supporting Information. Analogous models were refined against neutron diffraction data collected in the temperature range $5 < T/K < 388$. Figure 4b shows a plot of the refined ordered moment as a function of the temperature, indicating a magnetic ordering temperature of $T_N \sim 378(10)$ K for $Sr_3Fe_2O_4Cl_2$. Due to the presence of metallic iron in the sample, it was not possible to confirm the magnetic ordering temperature from susceptibility measurements.

Discussion

The topotactic reduction of $Sr_3Fe_2O_5Cl_2$ with LiH results in the deintercalation of oxide ions from the SrO layer of the

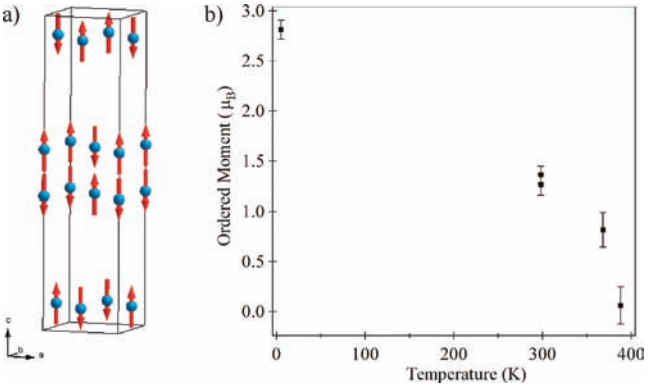

Figure 4. (a) The G-type antiferromagnetic model refined for $Sr_3Fe_2O_4Cl_2$. (b) A plot of the refined magnetic moment per iron center as a function of the temperature for $Sr_3Fe_2O_4Cl_2$, indicating a magnetic ordering temperature of $T_N \sim 378$ K.

material and the formation of $Sr_3Fe_2O_4Cl_2$, as shown in Figure 5. Bond valence sums (BVS)[11] calculated for the iron centers in $Sr_3Fe_2O_4Cl_2$ (Table 2) are consistent with the presence of Fe(II). In addition, they reveal that the long Fe−Cl bond (2.977(2)Å) contributes only 4.2% to the BVS total of the iron center, so the iron coordination geometry is effectively square-planar. There are relatively few examples in the literature of square-planar Fe(II) centers in extended solids for comparison. Those that are reported have been prepared by similar topotactic reduction syntheses as $Sr_3Fe_2O_4Cl_2$. $SrFeO_2$ for example has been prepared by the topotactic reduction of $SrFeO_{3-x}$ with CaH_2.[5] Comparison of the structural parameters of $Sr_3Fe_2O_4Cl_2$ and $SrFeO_2$ (Figure 6) reveals a remarkable similarity in the in-plane Fe−O bond lengths of 2.006(1) Å and 1.996(1) Å, respectively.[5]

Structural Selectivity. The reduction of $Sr_3Fe_2O_5Cl_2$ with LiH removes oxide ions exclusively from the axial AO layers of the host structure. This selectivity is in direct contrast to that shown by a number of other $AO(ABO_3)_n$ Ruddlesden−Popper oxides such as $LaSrCoO_4$ and $Sr_3Mn_2O_7$. During the topotactic reduction of these phases, anions are selectively deintercalated from the "equatorial" BO_{2-x} layers of their structures.[12,13] These contrasting selectivities can be rationalized by considering the different coordination requirements of the different cations in each system. Following the logic described previously,[9] and taking $Sr_3Fe_2O_5Cl_2$ as an example, it is clear that in order to best satisfy the competing coordination requirements of both strontium and iron cations on reduction, oxide ions will be removed from sites which form the strongest bonds to the iron and the weakest bonds to the strontium sites. We can evaluate this idea using bond valence sums (BVS)[11] as has been demonstrated previously for the $Sr_7Mn_4O_{15-x}$ phases.[9] BVS calculations can give a crude approximation of the cation−anion bond strengths in a solid and can thereby determine which anion is most likely to be deintercalated upon reduction. Contributions made by the iron and strontium cations to the BVS of the different anion sites in $Sr_3Fe_2O_5Cl_2$ are shown in Table 3. The largest value of Fe BVS − Sr BVS clearly predicts that

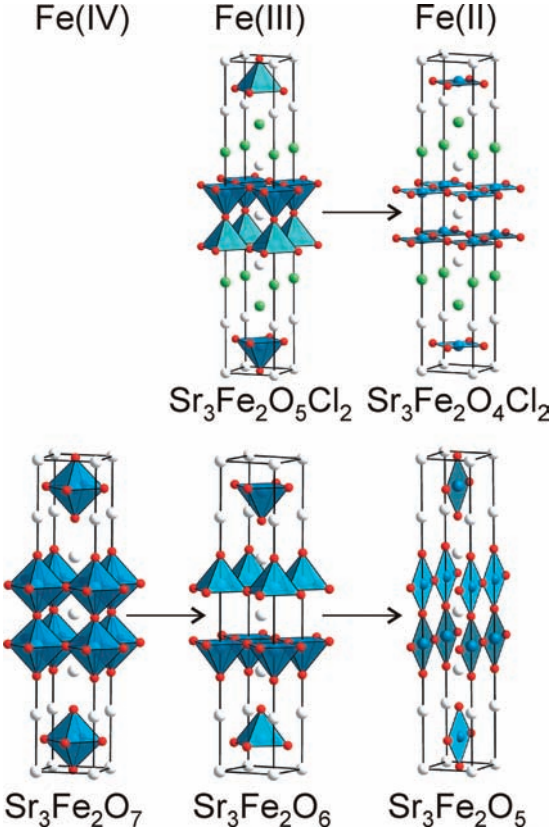

Figure 5. Reduction of $Sr_3Fe_2O_5Cl_2$ and $Sr_3Fe_2O_7$. The reduction of $Sr_3Fe_2O_5Cl_2$ proceeds via the removal of oxide ions from bridging axial sites to yield $Sr_3Fe_2O_4Cl_2$. The reduction of $Sr_3Fe_2O_7$ proceeds initially by the removal of ions from bridging axial sites to form $Sr_3Fe_2O_6$. A subsequent reduction step which involves the deintercalation of oxide ions from equatorial sites and a rearrangement of the anion lattice leads to the formation of the spin-ladder phase $Sr_3Fe_2O_5$.[13]

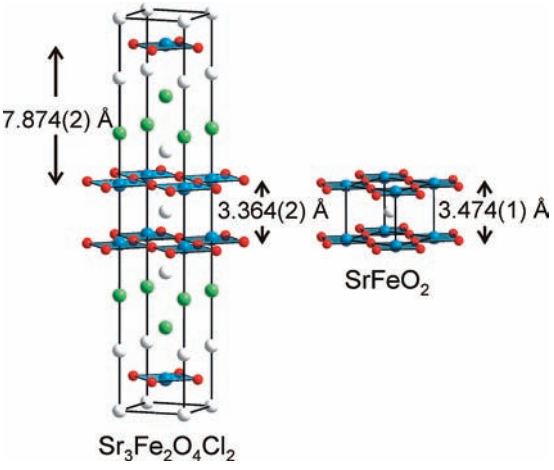

Figure 6. The structures of the topotactically reduced phases $Sr_3Fe_2O_4Cl_2$ and $SrFeO_2$, showing the different separations between the FeO_2 layers in each phase.

oxide ions will be removed from the O(1) "bridging axial" anion site on reduction in agreement with observation. Analogous calculations for $LaSrCoO_4$ and $Sr_3Mn_2O_7$ shown in the Supporting Information correctly predict the opposite selectivity, which is observed experimentally.[12,13]

The topotactic reduction of the all-oxide analogue of $Sr_3Fe_2O_5Cl_2$, $Sr_3Fe_2O_7$, provides another instructive

(11) Brese, N. E.; O'Keeffee, M. *Acta Crystallogr., Sect. B: Struct. Sci.* **1991**, *B47*, 192–197.
(12) Hayward, M. A.; Rosseinsky, M. J. *Chem. Mater.* **2000**, *12*, 2182–2195.

Table 3. Bond Valence Sums Calculated for the Anion Sites of $Sr_3Fe_2O_5Cl_2$

	O(1)	O(2)	Cl(1)
Fe BVS	**1.474**	1.068	0.086
Sr(1) BVS	**0.649**	0.235	
Sr(2) BVS		0.636	1.155
Fe BVS − Sr BVS Total	**0.825**	0.197	−1.069

comparison. As shown in Figure 5, the reduction of this phase occurs via a two-step process. Initially, oxide ions are deintercalated from the "bridging axial" anion sites in the host structure (in agreement with BVS predictions, as shown in the Supporting Information), leading to the formation of $Sr_3Fe_2O_6$, a structural analogue of $Sr_3Fe_2O_4Cl_2$. However, $Sr_3Fe_2O_6$ can be further reduced to a phase of composition $Sr_3Fe_2O_5$. BVS calculations, detailed in the Supporting Information, predict this reduction should occur via the removal of oxide ions from "equatorial" anion sites. However, the reduction is observed to progress with the removal of some equatorial oxide ions and a rearrangement of the anion lattice to yield a ladder-type structure incorporating pseudo-square-planar Fe(II) centers, as shown in Figure 5.[6] This anion lattice rearrangement suggests that the square-planar Fe(II) coordination formed is energetically preferable to the "tetrahedral" coordination that would result from the simple topotactic deintercalation of oxide ions from the equatorial layers of $Sr_3Fe_2O_6$. While it is clear that $Sr_3Fe_2O_6$ and $Sr_3Fe_2O_4Cl_2$ adopt strongly related structures, there is no evidence for a related reduction/rearrangement in the oxyhalide phase. This is unsurprising because the corresponding reduction would require the formation of an iron phase with an average oxidation state of below Fe +2. To the best of our knowledge, there are no known examples of a topotactic reduction resulting in the formation of iron with such an oxidation state. In addition, an analogous rearrangement of "$Sr_3Fe_2O_3Cl_2$" to a ladder-type structure is clearly less feasible than that of $Sr_3Fe_2O_5$, as this would leave the strontium cations within the SrCl rock salt layers (Sr(2)) significantly "under bonded" in large O_2Cl_5 coordination sites.

Chemical Selectivity. Complex transition metal oxyhalides provide an opportunity to evaluate the ability of the binary metal hydrides to selectively deintercalate different anion types. As described above, it is clear that during the reduction of $Sr_3Fe_2O_5Cl_2$ there is complete selectivity for the removal of oxide ions over chloride ions. This selectivity can be rationalized on the basis of two factors. In the specific case of $Sr_3Fe_2O_5Cl_2$, it can be seen from Figure 1 that each Sr(2) cation resides in a nine-coordinate coordination site of stoichiometry O_4Cl_5. BVS calculations performed for the $Sr_3Fe_2O_5Cl_2$ structure (Table 3) indicate that the chloride ions contribute only 4.2% of the total valence sum of the iron centers, but are "bonded" much more strongly to the Sr(2) cation. Removal of chloride ions from the structure of $Sr_3Fe_2O_5Cl_2$ as part of the reduction process would therefore have little effect on the iron centers but leave the coordination sphere of the Sr(2) cations exceptionally anion-deficient, contrary to the ideas of structural selectivity described above.

More generally, the removal of chloride ions from a complex oxyhalide would presumably occur via reaction 1, leading to the formation of LiCl, compared to reaction 2 for the removal of oxide ions, which leads to the formation of Li_2O as a byproduct.

$$Sr_3Fe_2O_5Cl_2 + x\cdot LiH \rightarrow Sr_3Fe_2O_5Cl_{2-x} + x\cdot LiCl + \frac{x}{2}\cdot H_2 \quad (1)$$

$$Sr_3Fe_2O_5Cl_2 + 2x\cdot LiH \rightarrow Sr_3Fe_2O_{5-x}Cl_2 + x\cdot Li_2O + x\cdot H_2 \quad (2)$$

Given that the conversion of LiH to Li_2O or LiCl provides the thermodynamic driving force for the topotactic reduction reactions, the greater lattice energy of Li_2O compared to LiCl (−2799 kJ mol^{-1} vs −834 kJ mol^{-1})[14] is clearly a deciding factor for the course of the reaction. This further suggests that in general we would expect to preferentially deintercalate oxide ions, rather than chloride ions, from the majority of complex oxyhalide hosts.

Magnetic Behavior. Neutron powder diffraction data show that $Sr_3Fe_2O_4Cl_2$ adopts a G-type antiferromagnetic arrangement below $T_N \sim 378$ K, exhibiting an ordered moment of 2.81(9) μ_B per iron center at 5 K. The magnitude of the ordered moment is consistent with a d^6 high-spin electronic configuration expected for Fe(II) ($S = 2, \mu_{ordered\_exp.} = 4\mu_B$) with a reduction in the observed moment due to covalency within the iron−anion contacts and/or slight disorder within the magnetic system. As a comparison, the isoelectronic and structurally similar infinite-layer phase $SrFeO_2$ (Figure 6) has an ordering temperature of $T_N \sim 473$ K and an ordered moment of 3.6 μ_B per iron center at 10 K.[5]

Neutron powder diffraction data also show that $Sr_3Fe_2O_4Cl_2$ retains tetragonal symmetry on cooling to 5 K. This indicates that in common with $SrFeO_2$, $Sr_3Fe_2O_4Cl_2$ does not have a degenerate electronic ground state, as such a state would be susceptible to a Jahn−Teller-like distortion.[15] This observation and the similarity of the iron coordination environments in the two phases make it reasonable to assume that the iron centers in $Sr_3Fe_2O_4Cl_2$ will adopt the same local orbital configuration as those in $SrFeO_2$. Previous reports on the electronic structure of $SrFeO_2$ indicate that the antiferromagnetic $S = 2$ ground state contains Fe(II) centers with an electronic configuration of: $(d_{z^2})^2(d_{xz}, d_{yz})^2(d_{xy})^1(d_{x^2-y^2})^1$.[5,15] Considering the Goodenough−Kanamori rules,[16] it can be seen that the transition metal d orbital expected to have the strongest contribution to the superexchange interactions is the $d_{x^2-y^2}$ orbital. Thus, the 180 °Fe $(d_{x^2-y^2})^1$ − O (2p) − Fe $(d_{x^2-y^2})^1$ superexchange interaction accounts for the strong antiferromagnetic coupling between iron centers within each FeO_2 layer of $Sr_3Fe_2O_4Cl_2$.

Coupling between FeO_2 layers is more complex. In the case of adjacent FeO_2 layers within $SrFe_2O_4$ blocks

(13) Gillie, L. J.; Wright, A. J.; Hadermann, J.; Van Tendeloo, G.; Greaves, C. *J. Solid State Chem.* **2003**, *175*, 188–196.

(14) *Handbook of Chemistry and Physics*, 89th ed.; CRC Press: Boca Raton, FL, 2008.

(15) Xiang, H. J.; Wei, S.-H.; Whangbo, M. H. *Phys. Rev. Lett.* **2008**, *100*, 167207.

(16) Goodenough, J. B. *Magnetism and the Chemical Bond*; Wiley: New York, 1963.

(Figure 6), direct Fe $(d_{z^2})^2$−Fe $(d_{z^2})^2$ exchange interactions result in G-type antiferromagnetic ordering. However, in order for the FeO_2 layers separated by SrCl rock salt layers to couple (Figure 6), a through-space mechanism must be employed if full three-dimensional antiferromagnetic order is to occur. The lower ordering temperature and smaller ordered moment observed for $Sr_3Fe_2O_4Cl_2$, compared to $SrFeO_2$, suggests that this through-space coupling is a limiting factor. The insertion of SrCl layers into the structure of $Sr_3Fe_2O_4Cl_2$ to form isolated double layer blocks and a more two-dimensional structure (Figure 6) leads to a reduction in the strength of the magnetic interactions between these double layer blocks (compared to the regularly spaced FeO_2 layers within the structure of $SrFeO_2$) and an associated lowering of both the magnetic ordering temperature and ordered moment.

The influence of dimensionality can also be seen in the magnetic ordering behavior of another isoelectronic phase, $Sr_3Fe_2O_5$. As shown in Figure 5, $Sr_3Fe_2O_5$ also contains Fe(II) centers in pseudo-square-planar coordination. However, in contrast to $SrFeO_2$ and $Sr_3Fe_2O_4Cl_2$, $Sr_3Fe_2O_5$ adopts a spin-ladder-type structure in which the dominant magnetic exchange pathways can be considered one-dimensional. Thus, it is no surprise that while $Sr_3Fe_2O_5$ adopts a similar magnetic structure to $Sr_3Fe_2O_4Cl_2$ it has a lower ordering temperature ("below 298 K").[6] Similar correlations between dimensionality and magnetic ordering temperatures are common in Ruddlesden−Popper systems, as exemplified by the increase in 3D magnetic ordering temperature when comparing $LaBaMnO_{3.5}$ to $LaSrMnO_{3.5}$ associated with the decrease in interlayer separation on the substitution of barium for strontium.[17]

(17) Kitchen, H. J.; Saratovsky, I.; Hayward, M. A. *Dalton Trans.* **2010**, *39*, 6098–6105.

Conclusion

In conclusion, we have demonstrated that binary metal hydrides can be used to selectively deintercalate oxide ions from complex transition metal oxychlorides. In addition, it can be seen that the topotactic reduction reactions of oxychlorides and isostructural complex oxides proceed to different extents to give isoelectronic phases with significantly different anion lattices (e.g., the two Fe(II) phases $Sr_3Fe_2O_4Cl_2$ and $Sr_3Fe_2O_5$ (Figure 5)). This suggests that by careful selection of substrate phases, the topotactic reduction of complex transition metal oxychlorides can lead to the preparation of novel anion-deficient phases with unique transition metal−oxygen sublattices which cannot be prepared via the reduction of all oxide substrates.

Acknowledgment. We thank R. Smith and E. Suard for assistance in collecting the neutron diffraction data. Experiments at the ISIS pulsed neutron facility were supported by a beam time allocation from the Science and Technology Facilities Council. E.D. thanks the EPSRC for a studentship.

Supporting Information Available: A complete description of the ordered magnetic model of $Sr_3Fe_2O_4Cl_2$. Observed, calculated, and difference plots from the structural refinement at 388 K, and the structural and magnetic refinement at 5 K of $Sr_3Fe_2O_4Cl_2$. Bond valence sum predictions for $LaSrCoO_4$, $Sr_3Mn_2O_7$, $Sr_3Fe_2O_7$, and $Sr_3Fe_2O_6$. This material is available free of charge via the Internet at http://pubs.acs.org.